

# Nanotech Net Working of New Materials using Pulsed Power Technology

Kiyoshi Yatsui, Hisayuki Suematsu, Chuhyun Cho, Makoto Hirai, Tsuneo Suzuki,  
and Weihua Jiang

Extreme Energy-Density Research Institute, Nagaoka University of Technology, Nagaoka 940-2188, Japan  
Fax: 81-258-47-9890 e-mail: yatsui@nagaokaut.ac.jp

Novel material preparation methods of pulsed wire discharge (PWD) and pulsed ion-beam evaporation (IBE) have been developed. By these methods, we have successfully synthesized novel materials including TiFe hydrogen absorbing alloy thin films and passivated transition metal nanosized powders, which have never or hardly been obtained by other methods. Thus, we think that the pulsed power technology can mend an open seam in the network of nanosized material preparation methods.

Key words: ion-beam evaporation, pulsed wire discharge, pulsed power technology, thin films, nanosized powders

## 1. INTRODUCTION

Many materials exhibiting novel functions have been found in the form of thin films and nanosized powders. Light emitting Si nanosized powders [1], Ba-Cu-O superconductor [2] and transparent p-type semiconductors [3] are good examples of the materials.

For preparation of the thin films or nanosized powders, the most widely used methods utilize condensation of vapor. In the vaporization, high energy which exceeds the heat of vaporization must be applied on either liquid or solid. If the energy is transferred to the liquid or solid for a long period, most of the energy will be dissipated as heat diffusion. Thus, heating in a short period assures high-energy-efficiency methods to produce vapor in the thin film or nanosized powder preparation. However, pulsed heating of the material was not widely studied for the preparation methods except for pulsed laser ablation. In the pulsed laser ablation, since the laser emission is a low-energy-efficiency process, overall energy efficiency is limited. Thus, development of other materials preparation methods using pulsed heating has been required.

Some of the authors have developed novel material synthesis methods utilizing pulsed power technology. The pulsed power technology had originally been developed for producing energy drivers in inertial confinement fusion apparatus. After the application of this technology to a field of material synthesis, a thin film preparation method of pulsed ion-beam evaporation (IBE) [4] and a nanosized powder synthesis method of pulsed wire discharge (PWD) [4-7] were developed. By these methods, pulsed and high-density plasma was formed and cooled either in gas or on substrates.

By using these methods, many novel materials have been synthesized. They are, for example, TiFe hydrogen absorbing alloy thin films and passivated transition metal nanosized powders, which had not been obtained by any other methods. In this review, experimental results on the preparation of the TiFe thin films and passivated transition metal nanosized powders

are described. From these results, characteristics of the IBE and PWD methods are unveiled.

## 2. PREPARATION OF TiFe HYDROGEN ABSORBING ALLOY THIN FILMS BY IBE

### 2.1 TiFe hydrogen absorbing alloys and the IBE method

Titanium iron (TiFe) is known as a hydrogen-absorbing alloy. When hydrogen atoms absorb and dissolve in the alloy, metal hydrides are formed. TiFe absorbs 1.8 wt.% of hydrogen [8] which is higher than those of some hydrogen absorbing alloys. Furthermore, TiFe is comparatively cheaper than other hydrogen absorbing alloys containing rare earth metals, such as LaNi<sub>5</sub> [8,9].

For applications in secondary batteries [10] and hydrogen separation membranes [11,12], hydrogen absorbing alloy thin films is being developed. Preparation of Ti-Fe thin films has also been attempted by a sputtering method. However, the thin films consisted of an amorphous Ti-Fe phase [8,9,13]. Since hydrogen absorption weight in amorphous Ti-Fe is less than that of crystallized TiFe [9], crystallization of TiFe thin films is required. However, crystallized TiFe thin films have not been obtained, to the best of the authors' knowledge.

Substrate heating or sample annealing may enhance the crystallization of the TiFe phase. However, oxidation of Ti must accompany because Ti is highly reactive. This would form secondary phases in the thin film. Thus, other methods, which enable us to prepare thin films at low temperature, have to be developed to obtain single-phase, crystallized TiFe thin films.

Thin films of TiFe are prepared by IBE. Crystallinity and surface morphology of the deposited thin films were studied by scanning electron microscopy (SEM) and X-ray diffraction (XRD).

### 2.2 Preparation of TiFe thin films by IBE

A schematic of the experimental setup for thin film preparation is shown in Fig. 1. The left-hand side represents an ion beam diode chamber, which produces a pulsed light ion beam (LIB), while the right-hand side

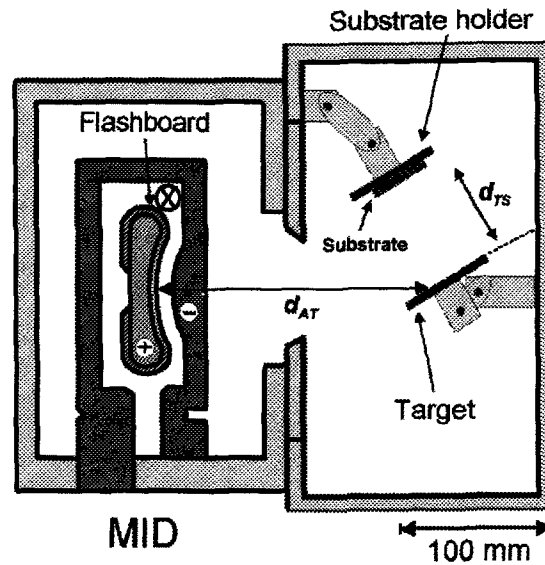


Fig. 1 Experimental setup for the preparation of TiFe thin films by IBE

represents the chamber to prepare thin films. The intense pulsed light ion beam generator "ETIGO-II" was utilized for the generation of the LIB [4]. The intense pulsed ion beam was extracted from the magnetically insulated diode (MID) with a geometrically focused configuration. The MID consists of an aluminum anode, on which the flashboard (1.5 mm polyethylene) was attached as the ion source, and the cathode with slits to extract the ion beam. The gap distance between the anode and the cathode is 10 mm. To achieve geometric focusing of the beam, the anode and the cathode were shaped as concave structures with curvature of 160 mm. The current supplied by the external slow capacitor bank produced a transverse magnetic field ( $\sim 1$  T) between the anode and the cathode, by which the electrons were magnetically insulated. The beams were mainly composed of protons ( $>75\%$ ) and some carbon ions.

Table I summarizes the experimental conditions. The target used was sintered TiFe bulks (Ti-50at.%Fe and Ti-40at.%Fe). Soda lime glass plates were used as substrates and were kept at room temperature. The

target was irradiated by the LIB and thin films were prepared without substrate heating. The chamber was evacuated to  $2 \times 10^{-4}$  Torr. The chemical composition of the targets and the thin films were determined by X-ray fluorescence analysis (XRF), energy-dispersive X-ray spectroscopy (EDS) and Rutherford backscattering spectroscopy (RBS). Target was also used as a standard sample for determining composition of the thin films by EDS. Phases in the thin films were identified by XRD with  $\text{CuK}\alpha$  radiation. Surface roughness ( $R_a$ ) of the thin film was measured with a roughness tester. Surface morphology of the thin films was studied by SEM.

Two thin films were deposited on the substrates after 3 shots of ion beam bombardments of the targets. Thickness of the thin films was approximately 400 nm. XRD patterns for the thin films are shown in Fig. 2. In a thin film prepared with a Ti-50at.%Fe target, some peaks including the strongest peak at  $43^\circ$  corresponds to those of TiFe phase. Peaks for  $\text{TiFe}_2$  and a small peak for Ti are also seen and indicate the presence of

Table I Experimental conditions

Target	Sintered TiFe (Ti-50 at.% Fe and Ti-40at.%Fe)
Substrate	Soda lime glass
$d_{AT}$	170 mm
$d_{TS}$	90 mm
Number of shots	3
Substrate temperature ( $T_S$ )	RT
Pressure	$2 \times 10^{-4}$ Torr

Table II Composition of thin film prepared with Ti-50at.%Fe target

Element	Composition (at.%)		
	XRF (Target)	EDS (Film)	RBS (Film)
Ti	49	44	50
Fe	51	56	50

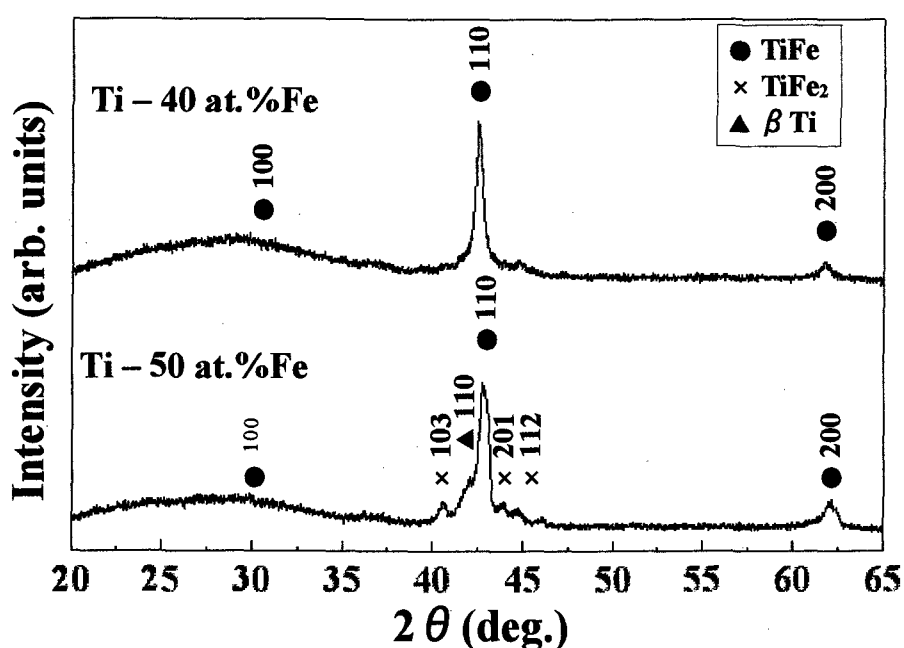


Fig. 2 XRD patterns for TiFe thin films prepared with Ti-50at.%Fe and Ti-40at.%Fe

secondary phases.

Average composition of the thin film prepared with a Ti-50at.%Fe target is shown in Table II. From the results by RBS and EDS, the Fe contents in the films were close to or slightly higher than those of the target. In order to decrease the Fe contents in the thin film, Ti rich target was used. The XRD pattern of a thin film prepared with a Ti-40at.%Fe target is also shown in Fig. 2. The peaks for  $\text{TiFe}_2$  and  $\beta\text{-Ti}$  are disappeared. Thus, a crystallized, single phase TiFe thin film was obtained for the first time.

Lattice parameters of the thin films were

determined from the peak position in Fig.2 to be 0.2990 and 0.3003 nm for thin films prepared with Ti-50at.%Fe and Ti-40at.%Fe targets, respectively. Relationship between composition and the lattice parameter of the quenched TiFe alloys has been reported [14] and is shown in Fig. 3. The lattice parameters of the thin films are also shown in Fig. 3. Using the relationship, Fe content in the TiFe phase is estimated to be 44 and 47at.% for thin films prepared with Ti-40at.%Fe and Ti-50at.%Fe targets, respectively. Both thin films consisted of Fe deficient TiFe compounds. This is the reason why secondary phases were formed in the thin film prepared using the stoichiometric TiFe target.

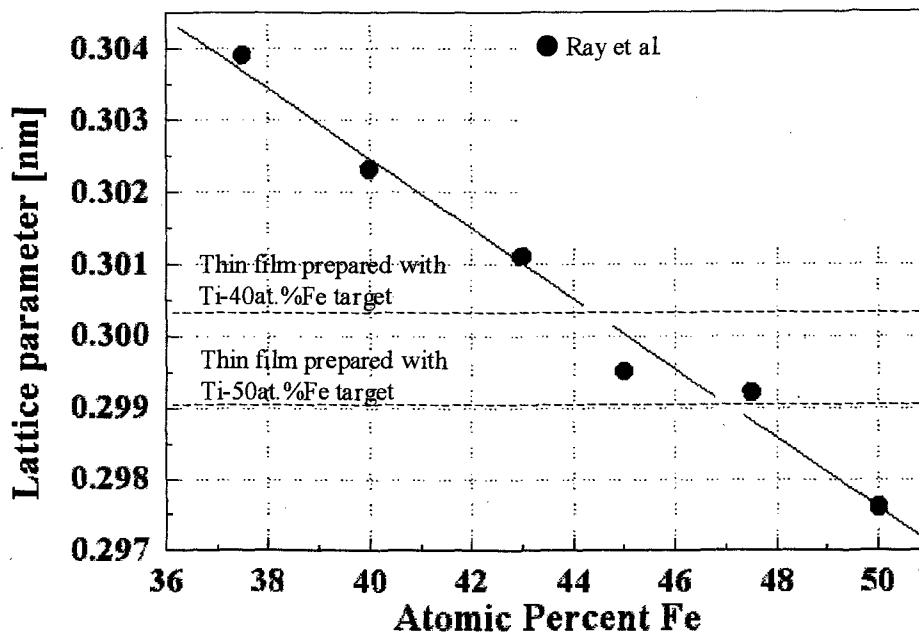


Fig. 3 Relationship between lattice parameter and composition in TiFe[17]

The TiFe phase is known to be stable between Ti-47.5at.%Fe and Ti-50.0at.%Fe at 1085 °C [14]. Compositions of the both TiFe compounds (Ti-44at.%Fe and Ti-47at.%Fe) are beyond the solubility. It implies that metastable TiFe phase and/or  $\beta$ -Ti phase, which could dissolve up to 22at.% of Fe, was formed because of the rapid cooling of the plasma on the surface of the substrates.

As mentioned before, no crystallized TiFe thin films had been obtained by any methods, while the first

TiFe thin films were successfully deposited at room temperature by IBE. The IBE method utilizes high-temperature and high-density plasma ( $10^{19}\sim 10^{20}/\text{cm}^3$ ) [15], which is higher than plasma densities in other methods. The mean-free-path of ions in the plasma is a few  $\mu\text{m}$ . It is difficult for atoms in the residual gas, i.e. oxygen, in the vacuum chamber to penetrate the plasma so that the thin films are not oxidized. At the same time, heat flux associated with the high-density plasma heats the substrate during the

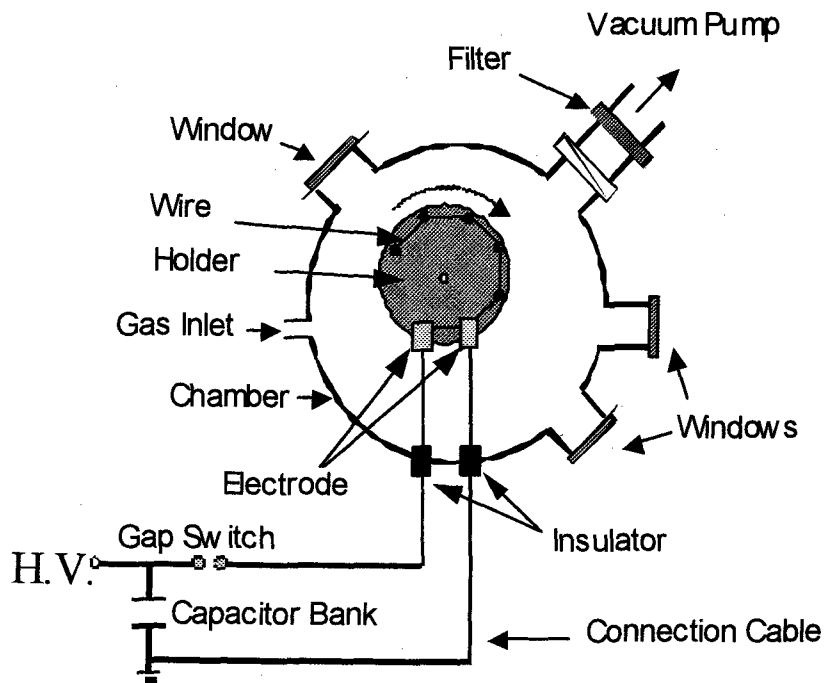


Fig. 4 Experimental setup of PWD apparatus

deposition [16]. The resulting temperature increase on the substrate surface enhances the crystallization. Furthermore, the temperature drops rapidly after the deposition. This quenching also prevents the oxidation of the thin films after the deposition. By these characteristics, crystallized TiFe thin films were successfully obtained by IBE.

### 3. PREPARATION OF PASSIVATED TRANSITION METAL NANOSIZED POWDERS BY PWD

#### 3.1 Passivated transition metal nanosized powders

Transition metal powders have been used in conductive pastes for various electronic devices. The most widely known application is electrodes in multi layer ceramic capacitors (MLCCs). Currently, powders of 0.5-1  $\mu\text{m}$  in diameter are used for mass production. For miniaturization of MLCC's size and deduction of their production cost, it has been required to produce thinner electrodes. On the other hand, the thicknesses of the electrodes are limited by the grain size of the metal powders. It would be beneficial for MLCC industries if nanosized powders of transition metal were available. However, it was difficult to obtain transition metal nanosized powders because of their quick oxidation in air. Thus, passivation layers on the surface of the transition metal particles are needed. Furthermore, for mass production of conductive pastes in the MLCCs, the passivation layer can be tailored to

disperse the particles in various chemical solvents. From the reasons above, no conventional methods met those requirements for the production of passivated transition metal nanosized powder for conductive pastes.

Pulsed wire discharge has been known as a novel nanosized powder preparation method using pulsed plasma [5-7]. In this method, no heat-treatments were required after the pulsed discharge in a chamber. If organic fume was filled in the chamber, it is expected that passivation layer can be formed after the discharge without degrading most of the organic molecules. Experimental results on the preparation of passivated Cu nanosized powders in organic fume and analysis of the passivation layer on the particles are described.

#### 3.2 Preparation of Cu nanosized powders

Experimental apparatus of PWD is shown in Fig. 4. Wires of Cu with diameters of 0.25 mm and with length of 25 mm were connected with electrodes in a chamber which was filled with nitrogen gas and mineral oil fume at a pressure of 750 Torr. The electrodes were also connected to a 10  $\mu\text{F}$  capacitor bank through a gap switch. Then, the capacitor was charged at the voltage of 5.2 kV. By closing the gap switch, pulsed current was driven through the wire. Typical pulse width was 10 to 20  $\mu\text{s}$ . The wire was evaporated by the Joule's heat. The metal vapor expanded and cooled in the gas to form nanosized powders. The powders floating in

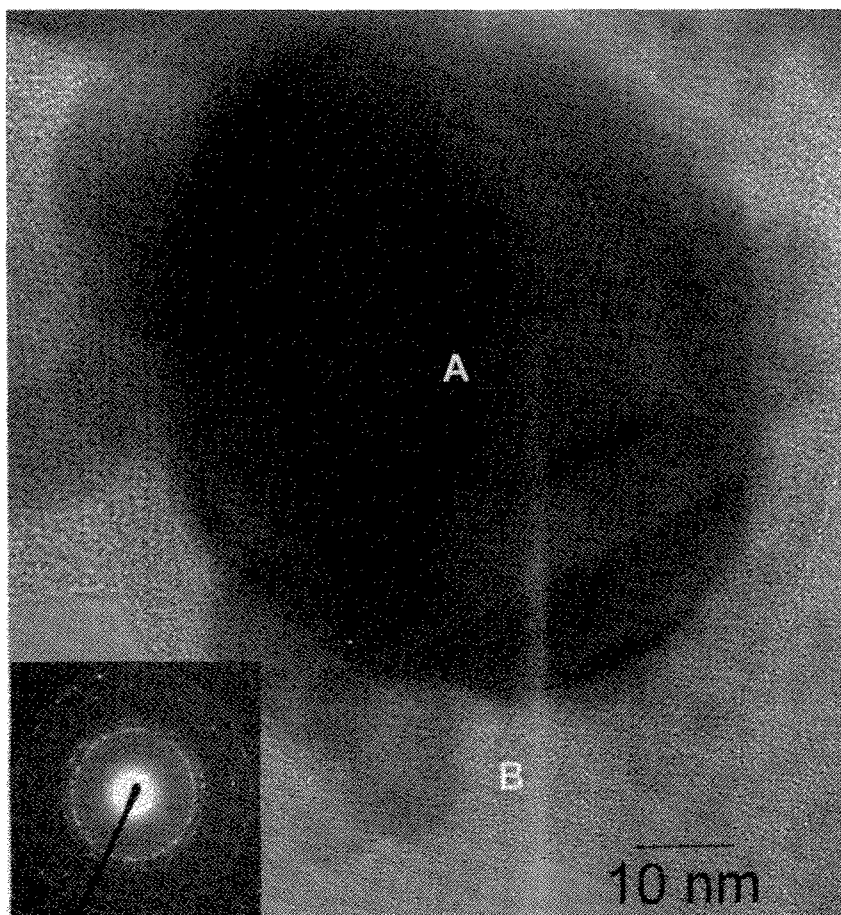


Fig.5 Bright field image of Cu particle and the selected area electron diffraction pattern

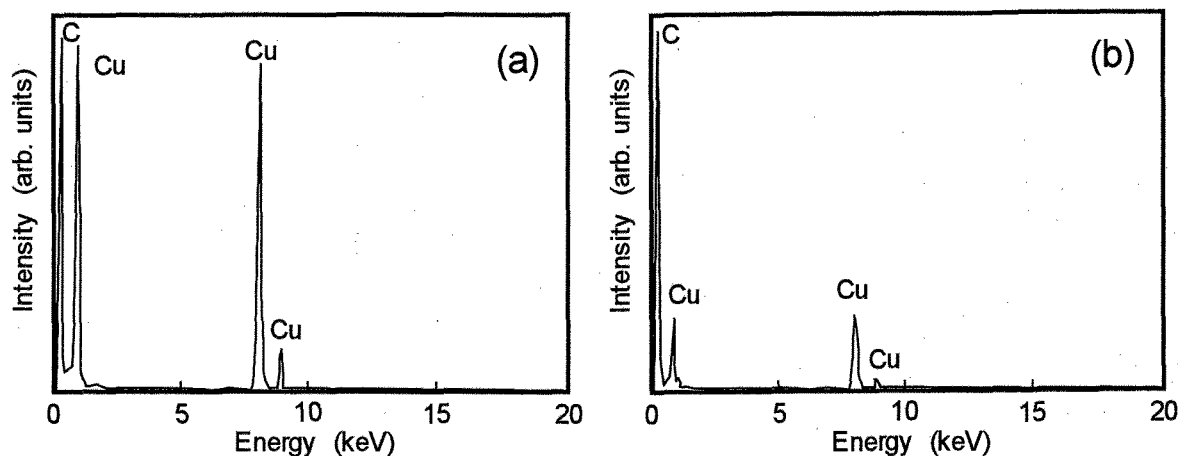


Fig. 6 EDX spectra at (a) point A and (b) point B in Fig. 5

the chamber were collected by pumping the oxygen gas through a membrane filter. The powders were observed by transmission electron microscopy (TEM). Powder was dispersed in acetone and was scooped on a holey carbon microgrid supported by a copper mesh. The TEM specimen was inserted in a transmission electron microscope (JEOL JEM-2010) operated at 200 kV. Composition of the powder was measured by energy dispersive X-ray analysis (EDX). The analyzer was attached on the transmission electron microscope. Phases in powders synthesized with different conditions were identified by selected electron diffraction (SAD).

A bright field image of a particle in Cu powder is shown in Fig. 5. A dark grain with diameter of 50 nm is seen. The inset in Fig. 5 is an SAD pattern for the powder. Most peaks correspond to those of Cu although faint peaks for  $\text{Cu}_2\text{O}$  are also seen. Spectra of EDX for points A and B in Fig. 5 are shown in Figs. 6 (a) and (b), respectively. At point A, strong two peaks for Cu are seen along with a peak for C. On the other hand, the Cu peaks at point B decreased while the intensity of the C peak is almost constant. From this result, we concluded that the Cu particle was coated by an organic layer. In Figs. 6 (a) and (b), no peaks for O are seen. Thus, this particle was not oxidized because of the presence of the organic layer, which worked as a passivation layer.

From these results, Cu nanosized powders were successfully coated by organic layers for passivation. In this process, various organic fumes can be introduced in the chamber so that the particles can be principally coated by any organic molecules. A novel passivated transition metal nanosized powder preparation method was developed.

#### 4. CONCLUSION

Experimental results have been successfully demonstrated on the preparation of crystallized TiFe thin films by pulsed ion beam evaporation technique and passivated Cu nanosized powders by pulsed wire discharge method. These characteristics are very unique, which have never been found by other methods.

#### 5. ACKNOWLEDGEMENT

This work was partly supported by the 21st Century COE Program of Ministry of Education, Culture, Sports, Science and Technology.

#### REFERENCES

- [1] L. T. Canham, *Appl. Phys. Lett.*, **57**, 1046-1048 (1990).
- [2] H. Yamamoto, M. Naito and H. Sato, *Jpn. J. Appl. Phys.*, **36**, L341-L344 (1997).
- [3] H. Kawazoe, M. Yasukawa, H. Hyodo, M. Kurita, H. Yanagi and H. Hosono, *Nature*, **389**, 939-942 (1997).
- [4] K. Yatsui, *Laser and Particle Beams*, **7**, 733-741 (1989).
- [5] M. Umakoshi, T. Yoshitomi and A. Kato, *J. Mater. Sci.*, **30**, 1240-1244 (1995).
- [6] Y. A. Kotov, E. I. Azaarkevich, I. V. Bektov, T. M. Murzakaev and O. M. Smatov, *Key Engineering Materials*, **132-136**, 173-176 (1997).
- [7] W. Jiang and K. Yatsui, *IEEE Trans. Plasma Sci.*, **26**, 1498-1501 (1998).
- [8] H. Tamura, *Hydrogen storage alloy -Fundamentals and Frontier Technologies* (N. T. S., 1998)[in Japanese].
- [9] K. Nakamura, *Script. Metal.*, **18**, 793-797 (1984).
- [10] T. Sakai, H. Ishikawa, H. Miyamura, N. Kuriyama, S. Yamada and T. Iwasaki, *J. Electrochem. Soc.*, **138**, 908-915 (1991).
- [11] G. Adachi, H. Nagai and J. Shoikawa, *J. Less-Common Met.*, **97**, L9-L10 (1984).
- [12] H. Sakaguchi, Y. Yagi, J. Shiokawa and G. Adachi, *J. Less-Common Met.*, **149**, 185-191 (1989).
- [13] K. Nakamura, *Ber Bunsenges Phys.Chem.*, **89**, 191-197 (1985).
- [14] R. Ray, B. C. Giessen and N. J. Grant, *Mettal. Trans.*, **3**, 627-629 (1972).
- [15] W. Jiang, C. Zhang, K. Masugata and K. Yatsui, *Jpn. J. Appl. Phys.*, **29**, 434-438 (1990).
- [16] W. Jiang, T. Suzuki and K. Yatsui, *Proc. 13th Int. Conf. Pulsed Power and Plasma Science*, **I**, 520-523 (2001).